CONF-780722--17

THE RESPONSE OF INCONEL 600 TO SIMULATED FUSION REACTOR IRRADIATION

F. W. Wiffen
Metals and Ceramics Division
Oak Ridge National Laboratory
Oak Ridge, TN 37830

June 1, 1978

Submitted for the ASTM — 9th International Symposium on Effects of Radiation on Structural Materials — Richland, Washington July 1978

Revised September 8, 1978

KEY WORDS: Radiation, irradiation, neutron irradiation, nickel-based alloys, austenitic alloys, radiation damage, tensile properties, ductility, fractography, swelling, swelling (helium bubbles), helium, displacement damage, thermal reactors, fusion reactors.

THE RESPONSE OF INCONEL 600 TO SIMULATED FUSION REACTOR IRRADIATION*

F. W. Wiffen
Metals and Ceramics Division
Oak Ridge National Laboratory
Oak Ridge, TN 37830

ABSTRACT

Inconel 600 was irradiated in HFIR to provide a partial simulation of fusion reactor service. Samples were irradiated at 55 to 700°C to investigate swelling and postirradiation tensile properties as a function of irradiation and test temperatures under conditions of concurrent displacement damage and helium production. Helium contents from 600–1800 appm and displacement levels of 4–9 dpa were achieved, and the results are used to estimate performance in a fusion reactor environment. The swelling was weakly dependent on temperature between 300 and 600°C, with swelling ranging from 0 to ∿1%, but increased rapidly above 600°. The swelling values were much larger than expected from fast reactor and ion bombardment results. Cold work was not effective in suppressing swelling of Inconel 600. Tensile property measurements and fractography on the same samples showed strength values increased for irradiation at 55 to 400°C but decreased below unirradiated values for irradiations at 600 and 700°C. Elongation values were lowest at the temperature extremes. Total elongations below 1% were only found for irradiation and test temperatures of 600 and 700°C. The fractures were completely transgranular for samples irradiated and tested at 300 and 400°C, of mixed mode but

*Research sponsored by the Office of Fusion Energy, U. S. Department of Energy under contract W-7405-eng-26 with the Union Carbide Corporation.

predominately intergranular at 500°C, and fully intergranular at 600 and 700°C. The results suggest that Inconel 600 does not offer any advantages over type 316 stainless steel and does not warrant further development for fusion reactor application.

INTRODUCTION

Among the large number of alloys that have been considered as candidate structural materials for first-wall and other components in the high-flux regions of fusion reactors are a number of nickel-base alloys. This interest in nickel alloys was first focused by the Princeton Plasma Physics Laboratory conceptual reactor study [1] which specified Nimonic PE-16 alloy as the structural material. The PE-16 structures were proposed for operation in the temperature range 250 to 600°C, with both low-stress components and highly stressed helium coolant tubes. PE-16 was selected as reference material in this reactor study on the basis of its resistance to swelling, relative to austenitic stainless steels, under both ion bombardment and fast reactor irradiation.

Previous ORNL work has shown that swelling under irradiation that partially simulates fusion reactor conditions can be quite different from swelling under fast reactor irradiation [2,3]. The differences, which arise from greater helium production rates under fusion reactor conditions, require that results from the fast breeder reactor radiation effects programs be used with caution in the fusion program. Further experimentation is required whenever better simulation of the fusion reactor environment becomes possible.

High Flux Isotopes Reactor (HFIR) irradiations were conducted to investigate radiation effects in nickel-base alloys under conditions of high-helium production rates accompanying the production of displacement damage. The alloys examined included Inconel 600, chosen as a typical solid solution strengthened nickel alloy. Inconel 600 has demonstrated swelling resistance under a limited range of irradiation conditions [4,5].

The goals of these experiments were: (1) to investigate swelling under conditions of concurrent displacement damage and transmutation helium production; (2) to examine tensile properties of these irradiated materials as a function of irradiation and test temperatures. Samples of Inconel 600 were included in both the solution-annealed and 20% cold-worked conditions.

The design of these experiments was based on experience gained in previous stainless steel irradiations performed in the Peripheral Target Position (PTP) of the HFIR flux-trap region. Irradiation temperatures ranged from 300 to 700°C. HFIR irradiation for 9000 MWd was planned to give helium contents in the range 600 to 1800 appm. Displacement levels ranged from 4 to 9 dpa.

Results reported here give swelling produced during irradiation, as measured by immersion density and changes in specimen length. Tensile properties of the same specimen are given for tests conducted at the irradiation temperature.

SIMULATION OF FUSION REACTOR CONDITIONS

Irradiation in HFIR provides a partial simulation of several of the important components of fusion reactor service conditions. The high nuclear heating rate in this reactor makes it possible to attain elevated temperatures in sealed irradiation capsules. Temperatures were selected to bracket possible application temperatures. The mixed neutron energy spectrum of HFIR results in displacement rates equal to or greater than proposed for fusion reactors (due to HFIR's fast neutrons) and very high helium production rates due to thermal neutron captures. Almost all the helium is produced in a reaction sequence believed to be unique to the major isotope of nickel:

$$^{58}Ni + n_{th} \rightarrow {}^{59}Ni + \gamma$$

$$^{59}Ni + n_{th} \rightarrow {}^{56}Fe + {}^{4}He \quad .$$

Since these two reactions have appreciable cross sections only for thermal energy neutrons, helium production from this sequence is important in thermal spectrum fission reactors but not in fast spectrum fission reactors nor in fusion reactors.

Table 1 gives a number of parameters for comparison of the response of Inconel 600 in a proposed fusion reactor to the response in the Experimental Breeder Reactor-II (EBR-II) and in HFIR. Both fission reactors provide a higher total neutron flux, and also higher rates of atom displacements, than for the same alloy in a Tokamak at a nominal neutronic wall loading of 1 MW/m^2. The two fission reactors produce hydrogen, from (n,p) and similar reactions, at approximately the same rate as the Tokamak with the power level listed. If defect production rates are compared in combination, however, the hydrogen production rate is too low. The ratio of appm hydrogen/dpa for a fusion reactor is 104; for the two fission reactors this ratio is only 30 and 48. It is suspected that these differences are not of primary importance.

Helium is known to have a major effect on the irradiation response of metals, and must be treated as thoroughly as possible in predicting irradiation effects in future power systems. In this regard, the two fission reactors are quite different. EBR-II produces too little helium to simulate fusion reactor condition, and in HFIR the non-linear helium production rate soon results in too much gas. The ratio of appm helium/dpa is 29 for a fusion reactor and is constant with service time in this system. In EBR-II the ratio is 2.1, also constant with time. In HFIR this ratio is much higher and is time-dependent. After 100 days of irradiation, the ratio is 235; after one year it has increased to 345.

The result of these considerations is that in Inconel 600 processes that are driven solely by dpa level can be adequately simulated in either HFIR or EBR-II. Processes driven solely by helium production can best be simulated in HFIR. For most processes, however, the ratio of helium-to-displacement level is likely to be important. For these cases, then, the properties after irradiation in HFIR and EBR-II provide extremes that can be used to fit correlation models in predicting fusion power reactor service.

EXPERIMENT

The rod stock of Inconel 600 was purchased from a commercial vendor, with the composition given in Table 2. The rod was reduced to 4.6 mm (0.180 in.) diameter by cold swaging, with intermediate recrystallization anneals. Cylindrical specimens were machined from the rod. (This specimen has a gage section 2 mm in diameter and 18 mm long.) Samples to be irradiated with a solution annealed microstructure were annealed in an argon atmosphere for 4 h at 1080°C and then furnace cooled.

HFIR irradiation experiments contain a single string of eleven specimens located on the axis of a 12.7 mm diameter sealed containment tube. The specimens are held in place by centering hubs, and specimen holder segments fill much of the remaining volume of the experiment. The temperature drop from the specimen irradiation temperature to the reactor coolant temperature is taken across the centering spur on the ends of the sample, the centering hub, and fins. The irradiation temperature at each position is fixed by the width of the gas gap between specimen and holder, and by the geometry of the centering fins. Similar experiments have been described in more detail previously [2].

A few samples of Inconel 600 were irradiated in the same reactor position at a temperature near 55°C. These samples were held in place in perforated tubes, with the samples in direct contact with the cooling water.

Density determinations were by the immersion technique, using water with a few drops of photoflow added to reduce surface tension. Repeat measurements on control samples showed a data spread of ±0.12% about the average density, suggesting at least this much uncertainty in any single measurement on the irradiated samples. As the irradiated samples were not electrochemically cleaned prior to density measurement the surface oxide film formed during irradiation could have a small effect on the measured density decrease.

Tensile tests were run on an Instron Universal Testing Machine, in a resistance heated furnace operating in air. The samples were held for a 15 minute equilibrium period at the test temperature before application of the load. All tests were run at a cross head speed of 0.002 in./min, for a nominal strain rate of 4.6×10^{-5} sec^{-1} (0.0028 min^{-1}). All stresses reported are based on the pretest specimen dimensions. Fracture diameters were measured after test but the difficulties in hot cell measurement of diameters, and of identifying the correct location to be measured on the sample make these reults of limited usefulness. The generally low ductilities also contribute to the difficulty in determining the reduction in area.

Selected fracture surfaces were examined in an SEM to characterize the fracture mode.

RESULTS

The swelling data obtained in these experiments are given in Table 3. Irradiation parameters listed include temperature, fast neutron fluence, dpa level, and helium content. The displacement damage (dpa) was calculated for the HFIR-PTP neutron spectrum using the IAEA Working Group recommended model [7]. The helium content was calculated from correlations developed [8] for helium production in ^{58}Ni irradiated in HFIR.

Swelling in Inconel 600 ranged from 0 to almost 4% for the irradiation conditions examined. The results are tabulated in Table 3 and shown graphically as a function of irradiation temperature in Fig. 1. The data in Fig. 1 are shown with helium levels indicated but are plotted without regard to fluence differences in different samples. Inspection of these data shows the following:

(a) Swelling values are very high for the dpa level. This establishes immediately that the helium production rates calculated for fusion reactors will result in swelling rates in Inconel 600 much greater than predicted by results obtained from nickel ion bombardment and from fast reactor neutron irradiation studies.

(b) Swelling in Inconel 600 increases as the helium content increases, for a fixed irradiation temperature. The exceptions to this, at 55 and 300°C, may reflect only the uncertainty in swelling measurements for these small swelling values.

(c) Cold working Inconel 600 is not very effective in suppressing swelling during irradiation with high helium production rates.

(d) Swelling under these irradiation conditions is only weakly dependent on temperature for irradiations between ∿55 and 600°C but increases markedly for irradiations at 650 and 700°C.

The Inconel 600 data would be more useful if they could be normalized so some consideration was given to a possible method of accounting for the different fluences at each irradiation temperature. The simplest assumption that can be made is that swelling at a fixed irradiation temperature is controlled by the helium content alone. If we further assume perfect gas law behavior and a constant concentration of equilibrium helium bubbles containing all the gas, then swelling (S) will be proportional to the 3/2 power of the helium concentration (C_{He}),

$$S \propto C_{He}^{3/2} .$$

The swelling data were normalized using this assumption to the average helium value of the high helium-content data. The normalized values are shown graphically in Fig. 2. They reinforce the conclusions drawn earlier on the temperature dependence of swelling.

The microstructure in samples solution annealed and then irradiated at 400 and 650°C are shown in Fig. 3. Irradiation at 400°C produced cavities with diameters in the range 4 to 17 nm but with few cavities at the upper end of this size distribution. These cavities were uniformly distributed throughout the sample, with grain boundary regions neither depleted nor enhanced in cavity populations. The dislocation structure in this sample was a high concentration of tangled loops and networks. Cavities in the sample irradiated at 650°C were considerably larger, with the range of diameters of matrix cavities 45 to 290 nm and with larger than average cavities on grain boundaries. This sample also contained a moderate concentration of network dislocations.

The tensile properties for all tested samples, and for control samples tested in the hot cell, are given in Table 4. Most of the irradiated samples were tested at the same temperature as the designed irradiation temperature. The properties for the 20% cold-worked Inconel 600 are plotted vs test temperature in Fig. 4. Values for unirradiated samples of the same material, tested in the hot cells under conditions identical to the irradiated sample tests, are plotted for comparison in Fig. 4. Figure 5 gives the properties of Inconel 600 irradiated in the solution annealed condition, and gives handbook values for hot-rolled Inconel 600 rod. A few samples irradiated at ∿55°C were tested at higher temperatures. The results of these tests are given in Fig. 6.

Strength values for the irradiated material show a much greater dependence on irradiation and test temperature than do the unirradiated strength values. Irradiation and testing at 55 to 400°C produce strength values that exceed both the yield and ultimate strength of control specimens. Uniform and total elongations are well below the control specimen values. At higher temperatures the strength values for irradiated samples fall below the control values. The sample of 20% cold-worked material irradiated at 700°C had strength only about 20% that of the control. In both cold-worked and solution annealed material the irradiated material showed lower ductility at high and low temperatures than at the intermediate temperatures.

Comparison of Figs. 4 and 5 show a great deal of similarity in the behavior of material either cold-worked or solution annealed before irradiation. The strength values of irradiated 20% cold-worked material are constantly 80 to 140 MPa greater than for solution annealed material irradiated and tested at the same temperatures, for temperatures in the range ∿55 to 600°C. The ductility values, too, are closely similar for the two preirradiation microstructural conditions.

The effect of fluence on the irradiation response of solution annealed Inconel 600 appears to be a function of temperature. Strength increases and ductility decreases with increasing exposure for irradiation at 300°C. At 500 and 600°C strength decreased with increasing exposure. At 500°C higher fluence resulted in higher ductility but at 600°C the ductility decreased as fluence increased.

Fracture surfaces of the irradiated and tested 20% cold-worked samples were examined by SEM. Representative fracture surfaces are shown in Fig. 7 and correlated with the total tensile elongation. Control samples and irradiated samples tested at 400°C or lower show features typical of a fully ductile fracture mode. The fractures were transgranular, with fracture surfaces largely covered with ductile dimples. Higher temperature fractures all exhibited some degree of grain decohesion. The fracture at 500°C was approximately 50% by grain boundary separation, with regions of tearing joining the exposed grain boundaries. At 600 and 700°C the failure was totally intergranular. Pore structures on grain boundaries of the sample tested at 700°C marked the sites of grain boundary helium bubbles in this sample.

There was no evidence of the channel fracture mode observed in stainless steels [9] in these experiments.

These results suggest that at this fluence different mechanisms are dominant at the low and high extremes of the temperature range investigated. At the lower temperatures, hardening due to displacement damage is probably the dominant mechanism. Irradiation strengthens the matrix above the control values, and the strengthening increases as the dpa level increases. It is not immediately apparent what role helium plays in this temperature range, although it is plausible that it serves to enhance the rate of defect cluster nucleation. HFIR irradiation with high helium generation rate would thus produce a finer scale distribution of microstructural defects than would equivalent dpa level irradiation without the accompanying high helium production rates. The fine-scale damage would be especially effective in hardening the matrix.

For temperatures in the 600—700°C range the helium is undoubtedly controlling the mechanical property response to irradiation. The helium promotes intergranular fracture in this temperature range and explains the decreasing ductility with increasing fluence (and hence increasing amounts of helium).

In the intermediate temperature range, 300 < T < 600°C, both lattice hardening and helium embrittlement should be operative and a more complex dependence of tensile properties on fluence and temperature can be expected.

Samples irradiated at ∿55°C and then tested at elevated temperatures showed a somewhat different behavior. For these samples, the strength in tests at 300°C was lower than for samples irradiated and tested at 300°C. The ductility was lower for the samples irradiated at the lower temperature. A test at 600°C of a sample irradiated at 55°C resulted in strength values higher than for samples both irradiated and tested at 600°C. The ductility was comparable to tests of samples irradiated at 600°C. Properties in tests at 300°C are probably controlled by matrix hardening from the irradiation produced microstructure. Differences in strength for the two irradiation temperatures may reflect a greater stability of the microstructure to deformation at the temperature at which it was produced, compared to the lower stability of the microstructure produced at ∿55°C and then tested at 300°C. The opposite strength effects at 600°C probably reflect the much larger fraction of the helium produced at 600°C that has reached grain boundaries, than for samples irradiated at 55°C and then heated to 600°C for testing.

DISCUSSION

(1) Swelling

Irradiation-produced swelling in Inconel 600 ranged between 0 and 4% for the irradiation variables examined. The swelling was small, ≤1.0%, for irradiation temperatures between 55 and 600°C. In this lower temperature range, the swelling was slightly temperature dependent. In the temperature range 600 to 700°C the swelling increased rapidly with increasing temperature. It is assumed that all swelling results from the accommodation of helium in equilibrium gas bubbles, as was the case for type 316 stainless steel with high helium contents [3].

Swelling increased as the fluence increased. The two data points at each temperature 400 to 700°C showed a greater than linear dependence of swelling on the helium content. The average exponent of the swelling dependence on helium content for these four data points is 1.53, in good agreement with the value 1.5 expected if the swelling is the result of equilibrium gas bubbles containing all the neutronically produced helium. This also assumes that the cavity concentration is independent of helium content at each temperature.

The magnitude of swelling found in these experiments is much larger than found under conditions producing higher dpa levels but with little or no helium in the metal. Bombardment with nickel ions [4,10] at 625 and 655°C and dpa levels to 140 produced from 0 to 0.6% swelling, and ranked the alloy as "very low swelling" compared to stainless steel.

In these HFIR irradiations, with the high helium contents more typical of fusion reactor conditions, comparable swelling occurred at less than 10 dpa.

Brager, *et al.* [5] have evaluated the swelling in Inconel 600 irradiated in EBR-II to 13—30 dpa in the temperature range 420 to 700°C. For these conditions, where helium production would be below 65 appm, swelling of less than 0.35% resulted. Furthermore, the swelling decreased with increasing temperature, with an upper temperature limit for cavity formation of about 610°C. Preirradiation cold-work of 50% also suppressed swelling relative to solution annealed material for the EBR-II irradiation.

All of this evidence supports the thesis that, in the presence of high helium production during irradiation, swelling of Inconel 600 is driven by the gas content. Control of swelling would thus require development and stabilization of a high concentration of cavities, since the swelling produced by equilibrium gas bubbles and a fixed gas concentration will decrease as the concentration of cavities increases [11]. The current results show that 20% cold-work is not effective in suppressing swelling.

(2) Tensile Properties and Fracture Mode

The tensile properties, combined with examination of fracture surfaces, suggest that the irradiation-produced helium in these samples dominates the mechanical properties for temperatures of 500°C or higher. Strength values of samples irradiated and tested at 500°C or higher fall below the strength values of control samples, and ductilities also are severely reduced. Ductilities at 500°C are near 5%, and the fracture surfaces show mixed intergranular separation and transgranular tearing. At higher temperatures the fractures become fully intergranular. The low stresses in tests at the highest temperatures thus reflect the low decohesion stress to separate grains and do not reflect the flow stress of the matrix material. In this temperature range 500 to 700°C the strength values are a strong function of temperature.

In the temperature range 55 to 300°C the yield and ultimate stress was insenitive to temperature. Both cold-worked and solution annealed materials were strengthened by the irradiation, and ductility values were reduced. This response suggests the classic irradiation hardening that results from displacement damage. In this range the influence of helium probably arises through its influence on the development of the damage microstructure, rather than through any direct influence on the deformation or fracture process.

The transition between these two behavior regimes probably occurs in the range 400–500°C but is not well defined by these experiments. Any transition temperature can also be expected to be a function of fluence.

The general strengthening and ductility reduction observed for the lower temperatures in these experiments is similar to results reported after EBR-II irradiation of the same alloy to about 1.5 dpa [12]. In the case of the same alloy irradiated in thermal spectrum reactors [13], but to lower fluences, a somewhat similar dependence of tensile properties on temperature was found. [The neutron spectrum for the reactor used in the latter experiments is not available. Significant helium production during irradiation seems likely, but the data needed for exact calculations of dpa and helium content are not available.] Claudson [13] evaluated property dependence on test temperature for fixed irradiation temperature. He reported more severe ductility loss for tests at 650°C than at lower temperatures. He also found the 650°C ductility loss to be relatively insensitive to irradiation temperature. The present experiments showed the same trend; irradiation at 55 and 600°C resulted in similar low values of postirradiation ductility in 600°C tests.

CONCLUSIONS

Irradiation of Inconel 600 to produce 4 to 9 dpa and helium contents of 600 to 1800 appm at temperatures in the range 55 to 700°C produce significant swelling and loss of postirradiation tensile ductility. Swelling is only slightly temperature dependent, and $\leqslant 1\%$ for temperatures from 55 to 600°C. Swelling increases rapidly with increasing temperature from 600 to 700°C. Strength values are above the strength of control samples for temperatures below about 450°C. For higher temperatures, the strength values drop well below the strengths of unirradiated material. Similarly, the elongation was most severely reduced for temperatures of 600 and 700°C.

These results show that the helium produced during irradiation drives the property changes. For temperatures below about 600°C, the swelling is small, but is much greater than would be produced in low-helium irradiations. The swelling is presumed to result from the microstructural accommodation of the gas in gas bubbles. At higher temperatures much greater swelling results, with up to 4% swelling at 700°C. For temperatures above about 500°C failure occurs by intergranular separation, and the low decohesion stress results in low stresses in tensile tests.

The helium domination of the irradiation response of this alloy requires caution in judging the irradiation response of candidate alloys based on limited simulation experiment data. In particular, the results of irradiations in "hard" neutron spectra or in heavy ion bombardments must be used with caution, since they generally lack the appropriate helium content of the sample.

The high helium production rate expected for Inconel 600 in service in a fusion reactor, and the serious effects of helium on the irradiation response and postirradiation properties of this alloy, do not make it an attractive candidate for fusion reactor structures. The lack of effectiveness of 20% cold-work in improving the postirradiation response was particularly surprising and discouraging, in view of the effectiveness of this treatment in 316 stainless steel. Inconel 600 has no advantage over type 316 stainless steel and does not warrant further development for fusion reactor application.

ACKNOWLEDGMENTS

Thanks are due B. L. Cox for assistance with much of the experimental part of this work, to R. S. Crouse for assistance with the SEM, and to E. A. Kenik for help with HVEM. Discussions with J. O. Stiegler and M. L. Grossbeck were helpful in preparation of the manuscript.

REFERENCES

[1] R. G. Mills, "A Fusion Power Plant," MATT-1050, August 1974, Princeton University Plasma Physics Laboratory.

[2] F. W. Wiffen and E. E. Bloom, "Effect of High Helium Content on Stainless-Steel Swelling," *Nuclear Technology*, 25, 113 (1975).

[3] P. J. Maziasz, F. W. Wiffen, and E. E. Bloom, "Swelling and Microstructural Changes in Type 316 Stainless Steel Irradiated Under Simulated CTR Conditions," *Radiation Effects and Tritium Technology for Fusion Reactors*, p. I-259, CONF-750989 (March 1976).

[4] W. H. Johnston, J. H. Rosolowski, A. M. Turkalo, and T. Lauritzen, "An Experimental Survey of Swelling in Commercial Fe-Cr-Ni Alloys Bombarded with 5 MeV Ni Ions," *J. Nucl. Mater.* 54, 24–40 (1974).

[5] H. R. Brager, J. L. Straalsund, and T. K. Bierlein, "Irradiation Swelling Resistance of Inconel 600," pp HEDL-77 to 87 in *Quarterly Progress Report Irradiation Effects on Reactor Structural Materials, November, December 1971, January 1972*, HEDL-TME 72-27.

[6] T. A. Gabriel, B. L. Bishop, and F. W. Wiffen, "Calculated Atom Displacement and Gas Production Rates of Materials Using a Fusion Reactor First Wall Neutron Spectrum," *Nuclear Technology* 38, 427–33 (1978).

[7] T. A. Gabriel, B. L. Bishop, and F. W. Wiffen, *Calculated Irradiation Response of Materials Using Fission Reactor (HFIR, ORR, and EBR-II) Neutron Spectra*, ORNL/TM-6361 (in preparation).

[8] F. W. Wiffen, E. J. Allen, H. Farrar, E. E. Bloom, T. A. Gabriel, H. T. Kerr, and F. G. Perey, "The Production Rate of Helium During Irradiation of Nickel in Thermal Spectrum Fission Reactors," (paper in preparation).

[9] R. L. Fish and C. W. Hunter, "Tensile Properties of Fast Reactor Irradiated Type 304 Stainless Steel," *Irradiation Effects on the Microstructure and Properties of Metals*, ASTM STP 611, American Society for Testing and Materials, 1976, pp. 119–138.

[10] A. F. Rowcliffe, S. Diamond, M. L. Bleiberg, J. Spitznagel, and J. Choyke, "Swelling and Irradiation Induced Microstructural Changes in Nickel-Based Alloys," *Properties of Reactor Structural Alloys After Neutron or Particle Irradiation*, ASTM STP-570, American Society for Testing and Materials, 1975, pp. 565–583.

[11] R. S. Barnes, "A Theory of Swelling and Gas Release for Reactor Materials," *J. Nucl. Mater.*, 11, 135–148 (1964).

[12] J. M. Steichen and R. L. Knecht, "LMFBR Structural Materials Applications," pp. C-5 to C-13 in *HEDL Quarterly Technical Report*, HEDL-TME-74-4 Vol. 1 (January 1975).

[13] T. T. Claudson, "Effects of Neutron Irradiation on the Elevated Temperature Mechanical Properties of Nickel-Base and Refractory Metal Alloys," *Effects of Radiation on Structural Metals*, ASTM-STP-426, American Society for Testing and Materials, 1967, pp. 67–94.

Table 1. Radiation Effects Parameters for Inconel 600 in a Tokamak, EBR-II, and HFIR

		Tokamak Fusion Reactor[a]	EBR-II[b]	HFIR[b]
Location		First wall	Midplane, row 2	Midplane, PTP
Power Level		1 MW/m^2	62.5 MW(th)	100 MW(th)
Neutron Flux				
∿14 MeV	$\times 10^{17}$ $n/m^2/s$	6.85	0	0
>0.1 MeV	$\times 10^{18}$ $n/m^2/s$	2.58	21.	14.
Total	$\times 10^{18}$ $n/m^2/s$	3.62	25.	52.
Displacements per year[c]	dpa	12.	41.	33.
Hydrogen per year[c]	appm	1250.	1240.	1580.
Helium[c]				
100 days	appm	94	24	2130
1 year	appm	343	87	11400

(a) Calculations from reference 6.

(b) Calculation from reference 7.

(c) All calculations are for a plant factor of 100%.

Table 2. Chemical Analysis of Inconel 600[a]

Composition in Weight Percent							
Fe	Cr	Ni	Mn	Ti	Al	Si	C
6.7	15.3	77.3	0.32	0.18	0.07	0.28	0.05

[a] Heat NX9929, Supplied from HEDL stock pile. Original vendor INCO-Huntington Alloys.

Table 3. Swelling of Inconel 600 Irradiated In HFIR

Irradiation Conditions				Solution Anneal		20% Cold Worked	
Temperature (°C)	Fluence >0.1 MeV (10^{25} n/m^2)	Displacement Level (dpa)	Helium (appm)	Density Decrease (%)	Geometry 3 ΔL/L (%)	Density Decrease (%)	Geometry 3 ΔL/L (%)
55	5	4.5	670	0.38	0.1		
55	9.6	7.3	1470	0.21	0.2		
55	13.6	10.9	2670	0.25	0.3		
55	12.4	10.0	2220			NA[a]	0.2
300	5.3	4.3	650	0.34	−0.23	0.12	0.08
300	9.7	7.9	1560	0.30	0.19		
400	5.6	4.4	670	0.23	−0.02	−0.04	−0.12
400	8.5	7.0	1270	0.48	0.25		
500	7.0	5.9	970	0.23	0.31	0.41	−1.28
500	10.4	8.5	1760	0.85	0.50		
600	7.5	5.9	970	0.61	0.87	0.63	1.45
600	9.9	8.1	1640	1.13	0.72		
650	10.6	8.7	1840	2.60	NA		
700	8.8	7.0	1300	2.36	NA	1.51	NA
700	10.4	8.5	1770	3.88	NA		

[a]NA — Not Available.

Table 4. Tensile Test Results for Inconel 600, Irradiated in HFIR

Irradiation			Tensile	Stresses		Elongation, %	
Temp (°C)	dpa	He (appm)	Temp (°C)	YS[b] MPa(ksi)	UTS MPa(ksi)	ε_{unif}	ε_{total}
			Cold Worked 20% Before Irradiation				
	Control		35	600 (87.1)	725 (105.1)	14.9	20.7
	Control		300	540 (78.38)	700 (101.57)	15.5	19.2
	Control		400	524 (76.0)	708 (102.7)	20.9	26.1
	Control		500	486 (70.48)	671 (97.35)	24.3	25.1
	Control		600	472 (68.4)	634 (92.0)	13.6	16.3
	Control		700	439 (63.74)	453 (65.75)	1.3	14.2
55	10	2220	35	880 (127.7)	919 (133.3)	7.2	10.1
300	4.3	650	300	924 (133.96)	925 (134.16)	0.8	4.2
400	4.4	670	400	699 (101.4)	780 (113.2)	4.3	6.7
500	5.9	970	500	419 (60.79)	528 (76.54)	5.5	6.4
600	5.9	970	600	314 (45.6)	320 (46.4)	0.43	0.68
700	7.0	1300	700	85.9 (12.46)	85.9 (12.46)	0	0
			Solution Annealed Before Irradiation				
55	7.3	1470	35	856 (124.1)	857 (124.3)	0.17	13.7
55	7.3	1470	300	709 (102.9)	741 (107.4)	11.8	14.8
55	10.9	2670	300	638 (92.6)	716 (103.8)	17.2	20.2
55	4.5	670	600	518 (75.2)	536 (77.8)	.97	1.82
300	4.3	650	300	847 (122.9)	850 (123.3)	3.3	7.0
300	7.9	1560	300	871 (126.4)	877 (127.2)	1.1	1.6
400	4.4	670	400	609 (88.3)	716 (103.8)	8.7	10.0
500	5.9	970	500	324 (46.99)	385 (55.78)	3.3	3.7
500	8.5	1760	500	263 (38.1)	367 (53.2)	6.5	6.8
600	5.9	970	600	187 (27.1)	251 (36.4)	2.6	3.1
600	8.1	1640	600	150 (21.7)	159 (23.1)	0.6	0.8
700	8.5	1770	700	113 (16.32)	113 (16.32)	0	0

[a] All tests at nominal strain rate of 0.0028 min^{-1}.

[b] 0.2% yield strength.

FIGURE CAPTIONS

Fig. 1 (ORNL-DWG 76-11170R) Measured Density Decrease for Inconel 600 Specimens Irradiated in the HFIR Reactor. Irradiation at the indicated temperatures produces 4 to 9 dpa, and the helium content, in appm, shown at each datum.

Fig. 2 (ORNL-DWG 76-11168) Swelling of Solution Annealed Inconel 600 Normalized to an Average Helium Content of 1541 appm He. The normalization assumed all swelling was due to helium bubbles, ideal gas behavior of the helium, and that for small variations in helium content the bubble concentration remains constant, at any temperature.

Fig. 3 [(a) YE-11597; (b) YE-11599] Microstructures in Inconel 600, Solution Annealed Before Irradiation. Note difference in magnification. (a) Irradiated at 400°C to 7.0 dpa and 1270 appm He. The swelling was 0.48%. (b) Irradiated at 650°C to 8.7 dpa and 1840 appm He. Swelling 2.6%.

Fig. 4 (ORNL-DWG 76-11741R) Tensile Properties of Irradiated Inconel 600, Cold-Worked 20% Before Irradiation. Samples were irradiated and tested at the indicated temperatures.

Fig. 5 (ORNL-DWG 76-11740R) Tensile Properties of Irradiated Inconel 600, Solution Annealed 4 h at 1080°C Before Irradiation. Samples were irradiated and tested at the indicated temperatures.

Fig. 6 (ORNL-DWG 78-6696) Tensile Properties of Irradiated Inconel 600, Solution Annealed Before Irradiation. These samples were irradiated at about 55°C. They were held 30 min at the test temperature before tests.

Fig. 7 (ORNL-DWG 78-8627) Ductilities and Associated Fractographs for Inconel 600, 20% Cold-Worked Before Irradiation.

ORNL-DWG 76-11170R

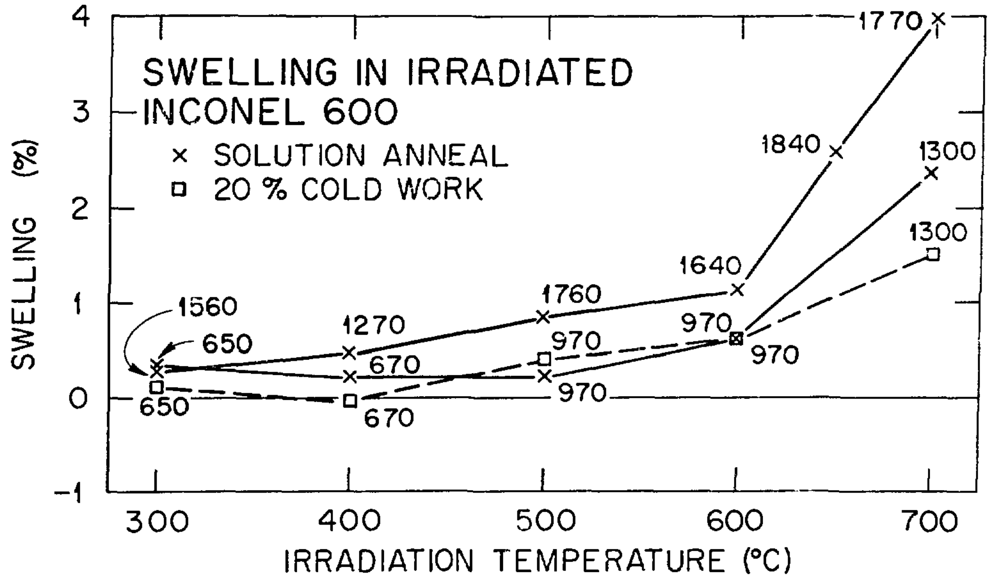

Fig. 1. Measured Density Decrease for Inconel 600 Specimens Irradiated in the HFIR Reactor. Irradiation at the indicated temperatures produces 4 to 9 dpa, and the helium content, in appm, shown at each datum.

ORNL-DWG 76-11168

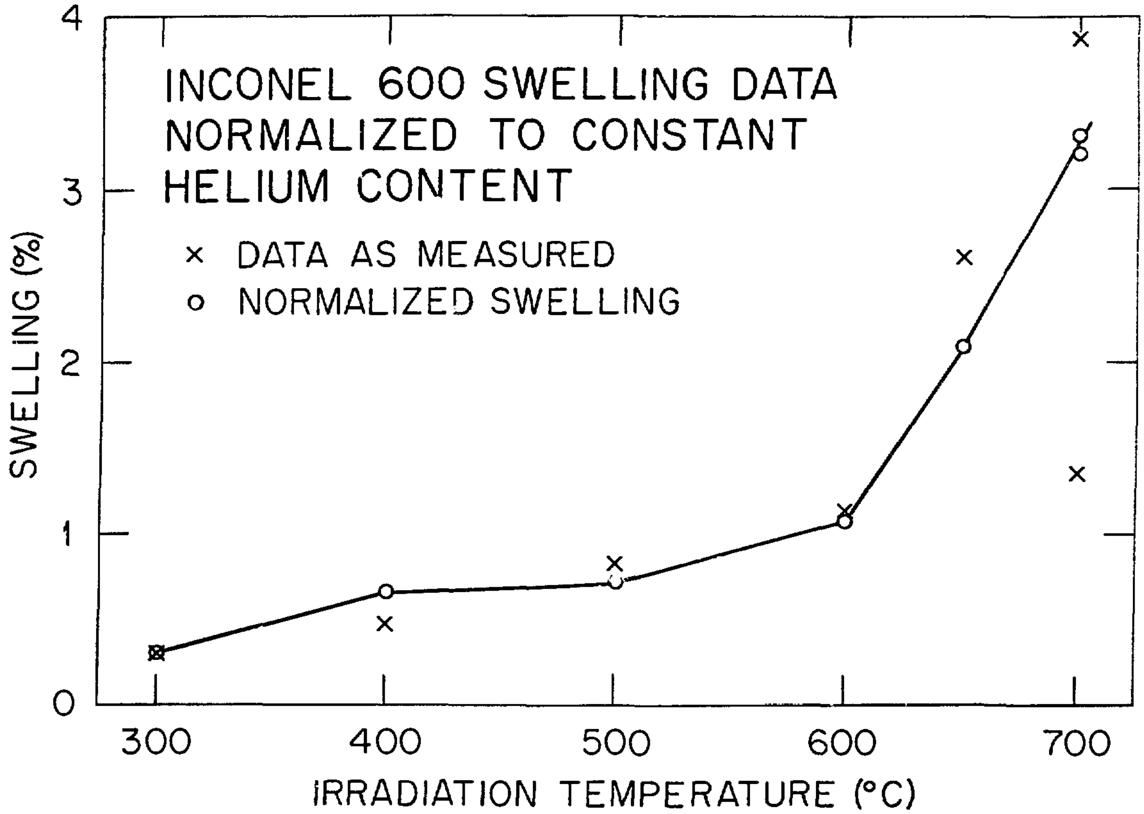

Fig. 2. Swelling of Solution Annealed Inconel 600 Normalized to an Average Helium Content of 1541 appm He. The normalization assumed all swelling was due to helium bubbles, ideal gas behavior of the helium, and that for small variations in helium content the bubble concentration remains constant, at any temperature.

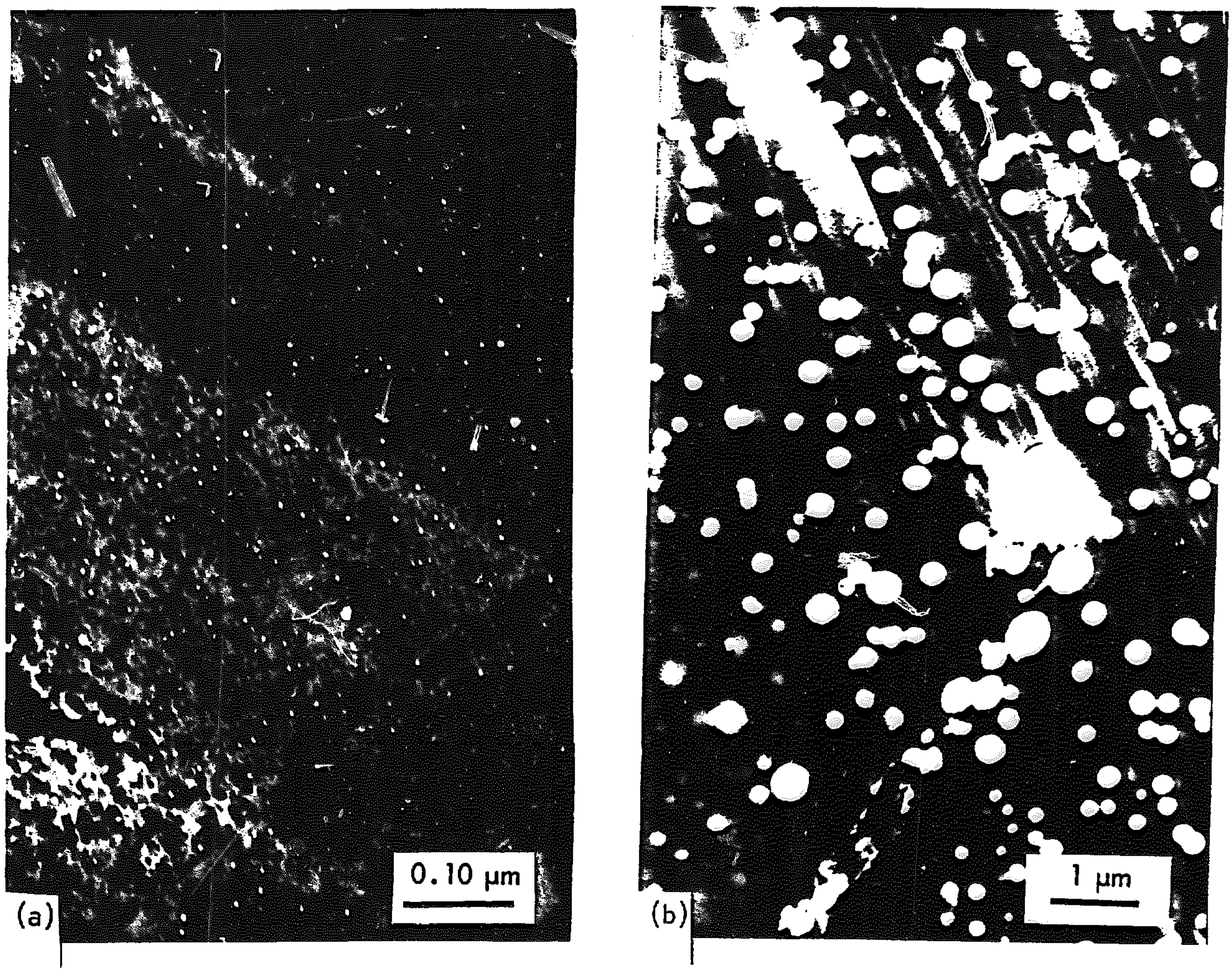

Fig. 3. Microstructures in Inconel 600, Solution Annealed Before Irradiation. Note difference in magnification. (a) Irradiated at 400°C to 7.0 dpa and 1270 appm He. The swelling was 0.48%. (b) Irradiated at 650°C to 8.7 dpa and 1840 appm He. Swelling 2.6%.

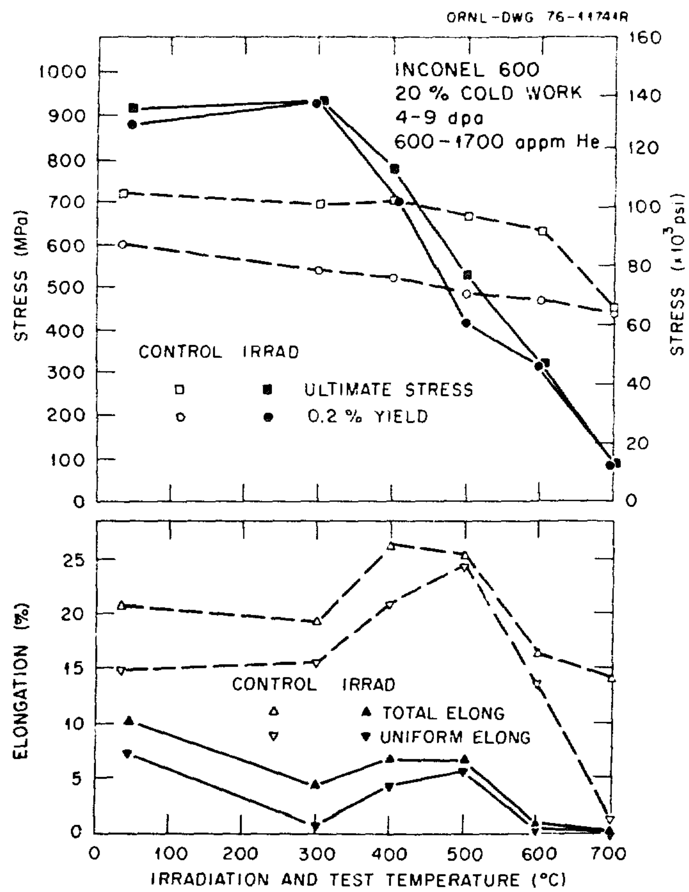

Fig. 4. Tensile Properties of Irradiated Inconel 600, Cold-Worked 20% Before Irradiation. Samples were irradiated and tested at the indicated temperatures.

Fig. 5, Wiffen, ORNL

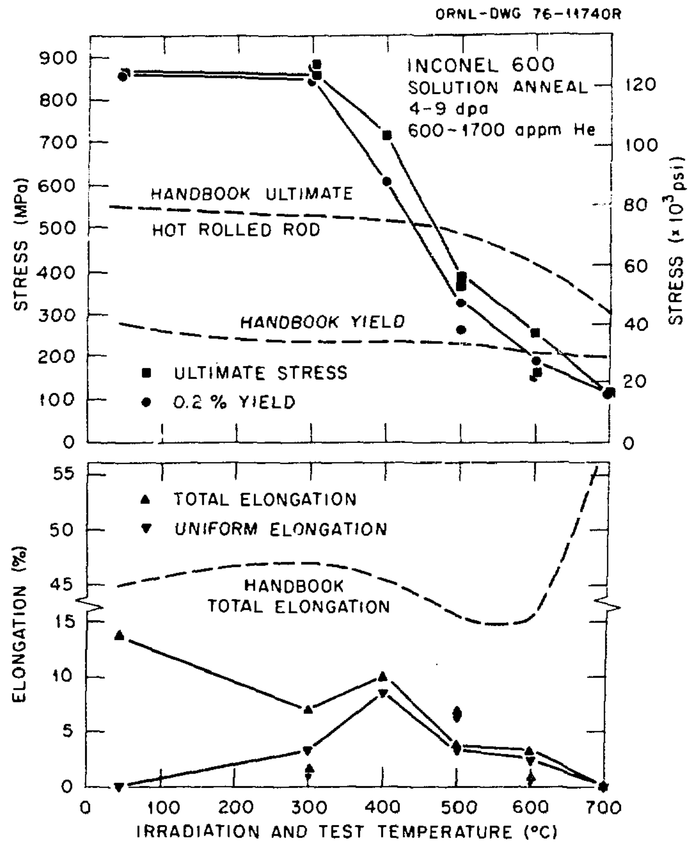

Fig. 5. Tensile Properties of Irradiated Inconel 600, Solution Annealed 4 h at 1080°C Before Irradiation. Samples were irradiated and tested at the indicated temperatures.

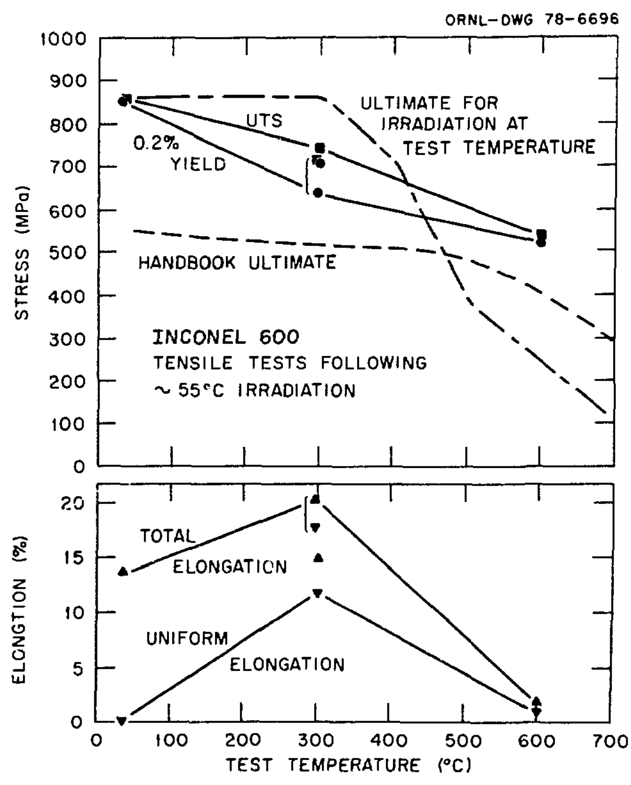

Fig. 6. Tensile Properties of Irradiated Inconel 600, Solution Annealed Before Irradiation. These samples were irradiated at about 55°C. They were held 30 minutes at the test temperature before tests.

ORNL-DWG 78-8627

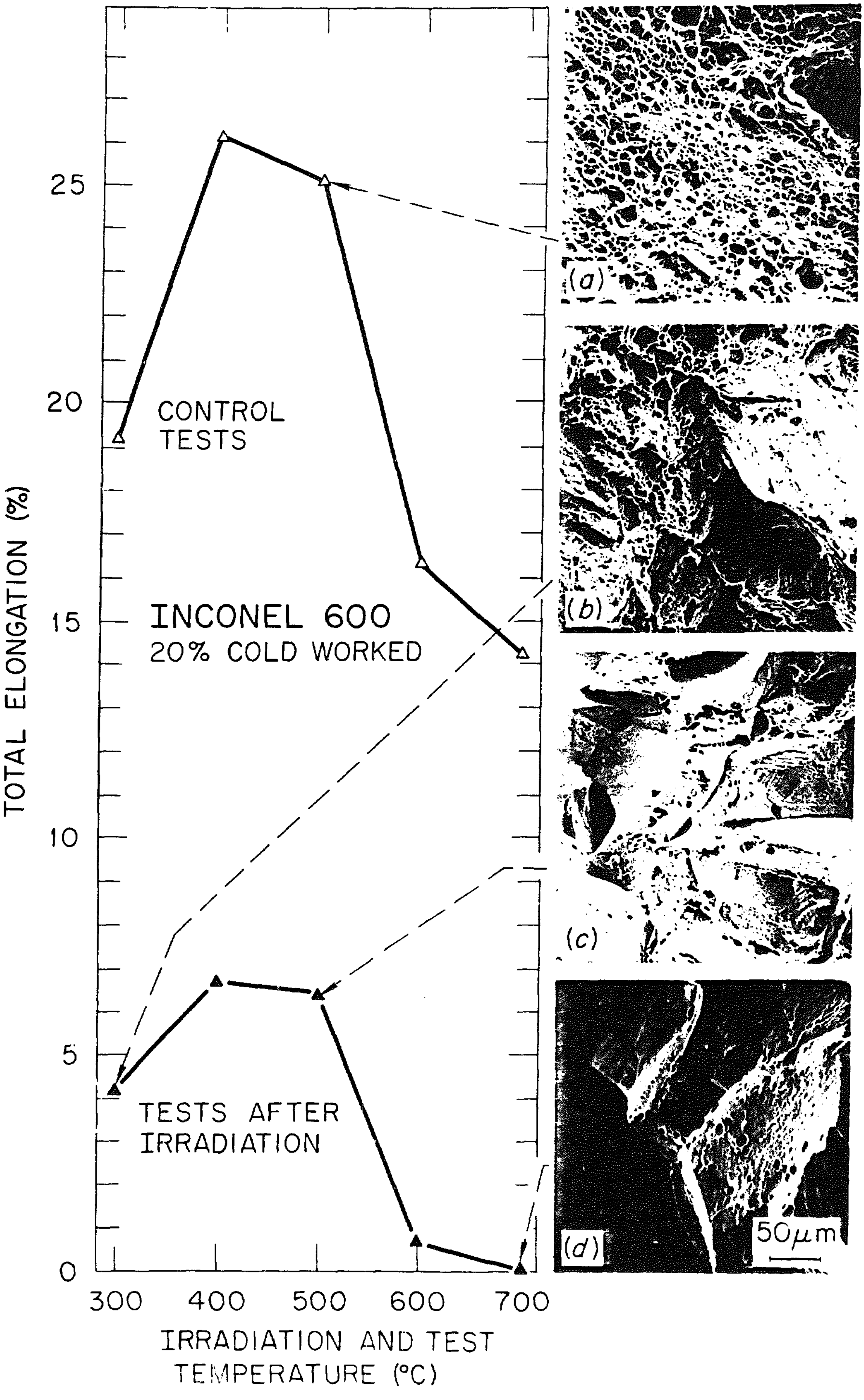

Fig. 7. Ductilities and Associated Fractographs for Inconel 600,